NANO LETTERS

2007
Vol. 7, No. 7
2000−2003

Charge State Control and Relaxation in an Atomically Doped Silicon Device

Søren E. S. Andresen,*[,†,‡] Rolf Brenner,[†,§] Cameron J. Wellard,[||,⊥] Changyi Yang,[||] Toby Hopf,[||] Christopher C. Escott,[†] Robert G. Clark,[†] Andrew S. Dzurak,[†] David N. Jamieson,[||] and Lloyd C. L. Hollenberg[||]

Australian Research Council Centre of Excellence for Quantum Computer Technology, University of New South Wales, Sydney, New South Wales 2052, Australia, and Australian Research Council Centre of Excellence for Quantum Computer Technology, University of Melbourne, Victoria 3010, Australia

Received April 4, 2007; Revised Manuscript Received May 22, 2007

ABSTRACT

We demonstrate time-resolved control and detection of single-electron transfers in a silicon device implanted with exactly two phosphorus donors. Charge state relaxation at millikelvin temperature is shown to be dominated by phonon emission and background charge fluctuations for low energies, while higher-order processes take over at higher energies. Our results reveal relaxation times for single-donor charge states of several milliseconds, which have significant implications for single-atom nanoelectronics.

As semiconductor devices approach the nanoscale, individual dopant atoms significantly impact on the electrical characteristics.[1] Devices with a precise number of dopants offer better control in this context and may offer pathways for new quantum devices based on the charge or spin states of single electrons.[2−7] Quantum control of the charge and spin states of individual electrons in solids plays a key role for realizing new electronic devices, e.g., in the context of quantum computing. Single-electron charging of metal nanodevices has been established for 2 decades,[8] but only recent reports have shown that single electrons confined in semiconductor quantum dots form quantum systems that can be manipulated coherently.[9−12] Several suggested schemes for silicon-based quantum computing rely on the control of single electrons on individual dopant atoms,[2−6] in which very long coherence times are possible.[7] Controlled single-ion implantation provides for atomic doping with reasonable positional accuracy,[13−16] but a fully scalable technology requires doping with true atomic precision.[17] Apart from quantum computing, such atomically engineered devices could also have more general impact for nanoscale electronics, e.g., for novel single-electron device applications.[18]

We use a single-ion implantation technique that relies on an active substrate configured as a $p-i-n$ detector with phosphorus doped (n-type) back-plane and boron doped (p-type) top electrodes on a masked, oxide-terminated, high-purity silicon substrate.[15] The electrodes, when reverse biased, allow counting of individual 14 keV phosphorus ions with over 94% confidence by detecting transients from impact-induced electron−hole pairs. The mask allows nanoscale positioning of the implant sites. As such, devices may be configured with exactly two phosphorus donors, implanted through two 15 nm diameter apertures, 50 nm apart.[16] Apart from aperture size, the positional accuracy is limited by straggling as well. We obtain a statistical estimate of the relative location of the two implants from Monte Carlo simulations based on SRIM.[19] These simulations indicate that the phosphorus ions penetrate through the 5 nm thermally grown, low interface trap density oxide, and 18 ± 10 nm into the high-purity silicon substrate. Assuming they impact through separate apertures, the donors will be configured 54 ± 15 nm apart. With equal probability, the ions will impact through the same aperture, in which case the separation will be 21 ± 11 nm. Activation by rapid thermal anneal (1000 °C, 5 s) may lead to diffusion by approximately 3 nm, as estimated from the intrinsic phosphorus diffusivity.[20] Defect-assisted diffusion, on the other hand, is very unlikely when implanting only two 14 keV phosphorus ions.

For read-out and control of its charge state, the two-donor structure is integrated with a single-electron transistor (SET) and a pulse gate (parts a and b of Figure 1), fabricated using a standard double-angle evaporation technique.[8] Radio frequency operated SETs (RF-SETs) have been established for some time as extremely sensitive and fast charge sensors approaching quantum-limited detection.[21] We make use of

* Corresponding author. E-mail: erfurt@nano.ku.dk.
† University of New South Wales.
‡ Present address: Niels Bohr Institute, Nano-Science Center, University of Copenhagen, Universitetsparken 5, 2100 København Ø, Denmark.
§ Present address: NXP Semiconductors Germany GmbH, General Application Discretes, Stresemannallee 101, D-22529 Hamburg, Germany.
|| University of Melbourne.
⊥ Present address: Walter and Eliza Hall Institute for Medical Research, Royal Melbourne Hospital, Victoria 3050, Australia.

10.1021/nl070797t CCC: $37.00
Published on Web 06/13/2007

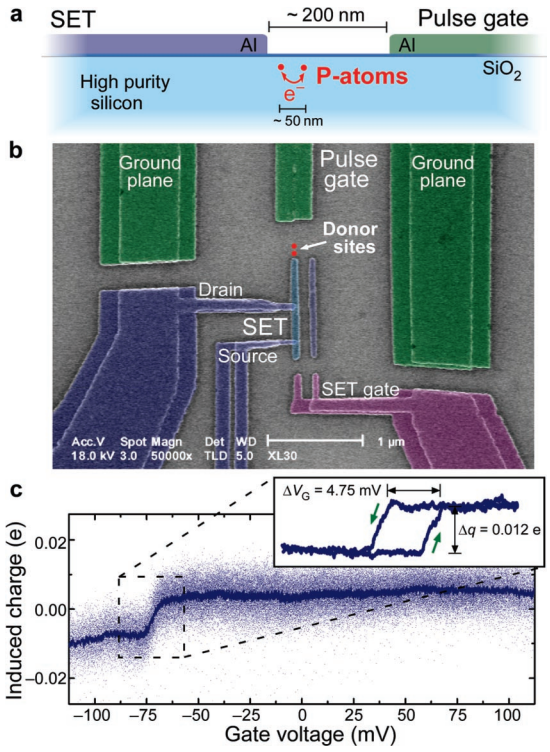

Figure 1. Two-atom device layout for voltage controlled charge transfer. (a) Schematic cross section of two-atom structure with pulse gate and single-electron transistor (SET) for charge state control and detection. (b) Scanning electron micrograph of coplanar gate line (green) and SET (blue) aligned with implant sites. SET tunnel junctions are formed using aluminum double-angle evaporation with an intermediate oxidation step. (c) Induced charge on SET island, measured at MHz bandwidth for several gate sweeps with averaged data in solid. Inset of averaged charge transfer shows hysteresis in gate voltage.

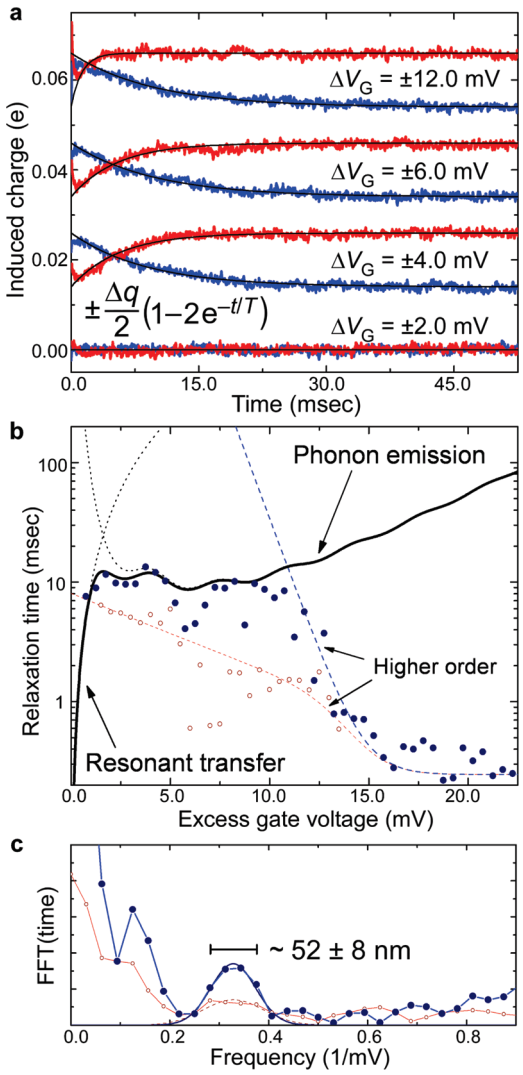

Figure 2. Time-resolved charge state relaxation. (a) Averaged traces of induced charge response after pulsing gate across hysteresis, $\pm\Delta V_G$ to negative/positive (blue/red). Fitted exponential decays are shown in black. (b) Relaxation time vs excess voltage of gate pulse to overcome hysteresis. Curve in solid black shows expected dependence for both resonant and phonon assisted transfer, assuming a donor separation of 50 nm. Each contribution appears in dashed black. Dashed red/blue indicates tendency for suppression at higher bias. (c) Fast Fourier transform (FFT) of bias-dependent relaxation time. Gaussian fits correspond to phonon interference for approximately 50 nm donor separation.

the RF-SET to detect voltage-controlled single-electron transfers in our two-donor structure. All our measurements are performed with a 340 MHz tank circuit resonator in a dilution refrigerator (50 mK), yielding a charge sensitivity of 15 $\mu e/\mathrm{Hz}^{1/2}$. Figure 1c shows the signature of a charge-transfer event in terms of induced charge on the SET island for gate voltage sweeps over a range of ±150 mV. The averaged trace reveals an induced charge signal of $\Delta q = 0.012e$, agreeing with previous RF-SET measurements on similar devices. Slightly different structures showed isolated events of $0.01-0.02e$ for transfers between less than ten donors,[16] and quasi-periodic signal of $0.02-0.05e$ for transfers between dots with hundreds of donors.[22] These results have also been confirmed by electrostatic modeling.[23] Measurements on an unimplanted control device showed no significant gate-controlled charge transfers.

Consequently, the measured Δq is consistent with single-electron transfer between two phosphorus donors in a singly charged configuration. The uncharged configuration is very unlikely due to the relative instability of the doubly occupied donor state (D^-). One of the donors is therefore likely to be ionized, either under the applied bias of ±150 mV or via electron capture by a nearby charge trap. This leaves the donor pair in a positively charged P_2^+ state with only one strongly bound electron. The hysteresis of several millivolts and offset to about −70 mV in gate bias may originate from a strongly coupled background charge. Most likely individual charge traps impose an additional bias, thereby stabilizing the system by responding to the donor pair charge state.

By applying pulsed gate voltages, we are able to directly observe the time response for single-electron transfers between the two phosphorus donors, from which we deduce the charge state relaxation time. Figure 2a shows averaged traces of the RF-SET induced charge signal for gate pulses applied with respect to the center of the previously identified charge-transfer hysteresis (Figure 1c). As expected, no transfer occurs when the pulse remains within the hysteresis. When pulsed gate voltages are applied outside the hysteresis, on the other hand, the averaged charge-transfer response gives rise to an exponential decay that fits well with the previously determined Δq, to determine the characteristic

decay time T. Repeating these measurements for different pulse amplitudes yields values for the charge state relaxation time over a range of gate bias values on both sides of the charge-transfer hysteresis (Figure 2b).

The data show remarkably long charge state relaxation times in excess of 10 ms and exhibit an asymmetry between the two sides of the transfer hysteresis. In order to analyze these values further, we apply a simple model that considers phonon emission,[24] and discuss the influence of background charge fluctuations. Relaxation rates due to both phonon emission and resonant transfer may be estimated using a hydrogenic model with coupling strength given by the symmetric−antisymmetric splitting

$$\Delta_{SAS} = 2E_0\left(1 + \frac{R}{a_B}\right)e^{-(R/a_B)} \quad (1)$$

where $E_0 = 45.5$ meV is the donor ground state energy, R is the donor separation, and $a_B = 3.1$ nm the renormalized Bohr radius. For fully incoherent resonant transfer, the relaxation rate is given by a Lorentzian line shape

$$\hbar\Gamma_{res} = \frac{\Delta_{SAS}}{1 + x^2} \quad (2)$$

Here, $x = \alpha e\Delta V_G/\Delta_{SAS}$ is the detuning away from the resonant bias condition, where α is a geometrical factor describing the ratio between the gate bias and the corresponding potential difference between the two donor sites. Combining the hydrogenic model with a simple deformation potential approach, the relaxation rate due to acoustic phonon emission is found to be[24]

$$\hbar\Gamma_{ph} = \frac{D^2q^3\left(1 - \frac{\sin qR}{qR}\right)}{4\pi\rho c_s^2(1 + x^2)\left(1 + \left(\frac{qa_B}{2}\right)^2\right)^4} \quad (3)$$

where silicon is assumed to have deformation potential $D = 3.3$ eV, density $\rho = 2.33$ g/cm^3, and speed of sound $c_s = 9.0$ km/s. Assuming a linear dispersion relation, the phonon wave number is given by $q = \Delta_{SAS}(1 + x^2)^{1/2}/\hbar c_s$.

Figure 2b shows a comparative plot of the experimental values against the predictions of the hydrogenic model including both resonant transfer and phonon emission. Here, the deduced relaxation times are plotted versus excess gate voltage to overcome the hysteresis, i.e., corrected for both size and position by simple translation. The modeled traces correspond to $R = 50$ nm, as expected for implants through separate apertures, and $\alpha = (50\text{ nm})/(225\text{ nm})$ as estimated from an effective length scale of 200−250 nm between gate and SET. Three-dimensional numerical modeling of the electrostatics with ISE-TCAD suggests $\alpha = 0.11$−0.23, depending on the exact geometrical configuration. At gate biases ranging up to 10 mV, the model resembles the data remarkably well, though for positive pulses, the relaxation time data seem suppressed by a factor of 2−5. For both pulse directions, the relaxation time falls off exponentially at higher gate bias and saturates at about 0.25 ms as marked in dashed red/blue.

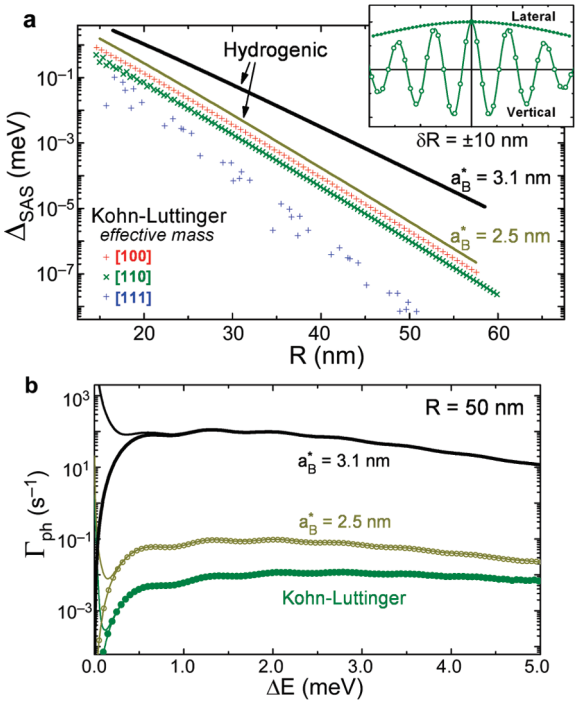

Figure 3. Hydrogenic contra Kohn−Luttinger model. (a) Coupling strength vs donor separation as predicted by hydrogenic ($a_B = 3.1$, 2.5 nm) and Kohn−Luttinger model (along [100], [110], and [111]). Insert shows variation for lateral and vertical displacement for 50 nm donor separation (along [110]). (b) Phonon emission rate vs detuning for 50 nm separation as predicted by hydrogenic and Kohn−Luttinger model (along [110]). Additional traces include the resonant Lorentzian contribution.

Considering the crudeness of the hydrogenic model, the quantitative agreement should only be regarded as an order of magnitude account. A much more complete treatment is achieved by adopting the Kohn−Luttinger formalism, previously used for calculating the coupling strength.[25,26] The results of both the hydrogenic model and the Kohn−Luttinger effective mass approach are shown in Figure 3a, both yielding an overall exponentially decaying $\Delta_{SAS}(R)$. Here, the Kohn−Luttinger results seem in much better agreement with the hydrogenic model assuming $a_B = 2.5$ nm. We note the erratic dependence on the exact atomic configuration for donor placements outside the (001) plane. We also adopted the Kohn−Luttinger formalism for evaluating the deformation potential matrix elements to give more realistic estimates of the relaxation by emission of acoustic phonons. Figure 3b shows the Kohn−Luttinger result together with the hydrogenic predictions, which seems in much better agreement for $a_B = 2.5$ nm. As such, the model assuming $a_B = 3.1$ nm most likely overestimates the coupling of donor states by at least an order of magnitude. Hence the data suggest that other channels contribute to the charge state relaxation, the most likely candidate being background charge fluctuations related to interface charge traps in the silicon dioxide.[27,28] Here, the asymmetry in pulse direction suggests a stronger coupling to one of the donors, probably due to microscopic coupling of a single charge trap. Nonetheless, the exponential scaling-factor e^{-R/a_B}, reflected to the fifth power in the relaxation rate, leads to the conclusion that the donors have indeed been implanted through separate aper-

tures, 50 nm apart. In fact, the full six-valley analysis in the Kohn−Luttinger formalism confirms that the time scales are commensurate with a donor separation of no less than 45 nm. The exponential roll-off versus gate bias beyond 10 mV is most likely a higher-order effect of excited donor states or coupling to the silicon conduction band. The saturation for large pulse voltages simply reflects the limited 10 kHz measurement bandwidth.

An important model-independent feature is the oscillatory behavior from interference between donor separation and phonon wavelength. Indeed, the data seem to replicate these oscillations, and a Fourier analysis is carried out to quantify this behavior (Figure 2c). The Fourier transformed relaxation time data exhibit a number of peaks versus frequency in gate voltage, most pronounced for 0.32 and 0.16 mV^{-1}. The broad peak around 0.32 mV^{-1} is consistent with oscillations due to phonon interference. The narrow peak at 0.16 mV^{-1} is attributed to a double period, manifested also as sharp minima for every second oscillation in Figure 2b. Interference with phonon wavelength occurs at a frequency in gate voltage related to the donor separation by $f_V = (\alpha e/hc_s)R$. Gaussian fits indicate a donor separation of 52 ± 8 nm, agreeing well with 54 ± 15 nm as expected for dopants implanted through separate apertures. The apparent double period is not predicted by the hydrogenic model, possibly due to the isotropic approximations in terms of effective mass, deformation potential, and phonon dispersion. Weaker occurring peaks for positive opposed to negative gate bias is consistent with background charge fluctuations coupled more strongly to one of the donors, as previously discussed.

Our combined results suggest that we are indeed studying single-electron transfers between the two phosphorus donors in our atomically doped silicon device. Although we cannot altogether exclude charge traps as the origin of the observed charge-transfer signal, the remarkable agreement with both theory and previous results indicates that we are most likely controlling the singly charged donor pair charge state. We observe remarkably long charge state relaxation times of the order 10 ms, simply reflecting that the coupling strength is exponentially suppressed with increasing separation, on a characteristic length scale given by the Bohr radius. As such, this specific two-donor structure is not suited for coherent manipulation which would require a separation of less than 35 nm to achieve a coupling stronger than any realistic rate of decoherence. On the other hand, our results hold promise for other novel concepts based on charge states of individual dopant atoms. The long relaxation time of several milliseconds outside the gate hysteresis presumably helps to keep the charge state pinned inside the hysteresis, even in a fluctuating charge background. Thus no transfers were observed inside the gate hysteresis, even for the longest measurements performed over time scales of several seconds.

Acknowledgment. The authors thank Sean Barrett, Gerard Milburn, Andrew Ferguson, and Jeffrey McCallum for fruitful discussions and Eric Gauja, Grigori Tamanyan, Robert Starrett, and David Barber for technical support. The work is funded by the Australian Research Council, the Australian Government, and by the US National Security Agency and US Army Research Office under Contract No. W911NF-04-1-0290.

Supporting Information Available: Further information regarding single-ion implantation, RF-SET charge sensing, the phonon emission theory, the coupling to background charge, as well as electrostatic modeling. This material is available free of charge via the Internet at http://pubs.acs.org.

References

(1) International Technology Roadmap for Semiconductors. *ITRS.net*, 2005.
(2) Kane, B. E. *Nature* **1998**, *393*, 133−137.
(3) Vrijen, R.; Yablonovitch, E.; Wang, K.; Jiang, H. W.; Balandin, A.; Roychowdhury, V.; Mor, T.; DiVincenzo, D. *Phys. Rev. A* **2000**, *62*, 012306.
(4) Hollenberg, L. C. L.; Dzurak, A. S.; Wellard, C.; Hamilton, A. R.; Reilly, D. J.; Milburn, G. J.; Clark, R. G. *Phys. Rev. B* **2004**, *69*, 113301.
(5) Hill, C. D.; Hollenberg, L. C. L.; Fowler, A. G.; Wellard, C. J.; Greentree, A. D.; Goan, H.-S. *Phys. Rev. B* **2005**, *72*, 045350.
(6) Hollenberg, L. C. L.; Greentree, A. D.; Fowler, A. G.; Wellard, C. J. *Phys. Rev. B* **2006**, *74*, 045311.
(7) Tyryshkin, A. M.; Lyon, S. A.; Schenkel, T.; Bokor, J.; Chu, J.; Jantsch, W.; Schäffler, F.; Truitt, J. L.; Coppersmith, S. N.; Eriksson, M. A. *Physica E* **2006**, *35*, 257−263.
(8) Fulton, T. A.; Dolan, G. J. *Phys. Rev. Lett.* **1987**, *59*, 109−112.
(9) Hayashi, T.; Fujisawa, T.; Cheong, H. D.; Jeong, Y. H.; Hirayama, Y. *Phys. Rev. Lett.* **2003**, *91*, 226804.
(10) Petta, J. R.; Johnson, A. C.; Marcus, C. M.; Hanson, M. P.; Gossard, A. C. *Phys. Rev. Lett.* **2004**, *93*, 186802.
(11) Petta, J. R.; Johnson, A. C.; Taylor, J. M.; Laird, E. A.; Yacoby, A.; Lukin, M. D.; Marcus, C. M.; Hanson, M. P.; Gossard, A. C. *Science* **2005**, *309*, 2180−2184.
(12) Koppens, F. H. L.; Buizert, C.; Tielrooij, K. J.; Vink, I. T.; Nowack, K. C.; Meunier, T.; Kouwenhoven, L. P.; Vandersypen, L. M. K. *Nature* **2006**, *442*, 766−771.
(13) Schenkel, T.; Persaud, A.; Park, S. J.; Nilsson, J.; Bokor, J.; Liddle, J. A.; Keller, R.; Schneider, D. H.; Cheng, D. W.; Humphries, D. E. *J. Appl. Phys.* **2003**, *94*, 7017−7024.
(14) Shinada, T.; Okamoto, S.; Kobayashi, T.; Ohdomari, I. *Nature* **2005**, *437*, 1128−1131.
(15) Jamieson, D. N.; Yang, C.; Hopf, T.; Hearne, S. M.; Pakes, C. I.; Prawer, S.; Mitic, M.; Gauja, E.; Andresen, S. E.; Hudson, F. E.; Dzurak, A. S.; Clark, R. G. *Appl. Phys. Lett.* **2005**, *86*, 202101.
(16) Mitic, M.; Andresen, S. E.; Yang, C.; Hopf, T.; Chan, V.; Gauja, E.; Hudson, F. E.; Buehler, T. M.; Brenner, R.; Ferguson, A. J.; Pakes, C. I.; Hearne, S. M.; Tamanyan, G.; Reilly, D. J.; Hamilton, A. R.; Jamieson, D. N.; Dzurak, A. S.; Clark, R. G. *Microelectron. Eng.* **2005**, *78*−*79*, 279−286.
(17) Schofield, S. R.; Curson, N. J.; Simmons, M. Y.; Rueβ, F. J.; Hallam, T.; Oberbeck, L.; Clark, R. G. *Phys. Rev. Lett.* **2003**, *91*, 136104.
(18) Likharev, K. K. *Proc. IEEE* **1999**, *87*, 606−632.
(19) *SRIM.org*; Ziegler, J. F.; Biersack, J. P.; Littmark, U. *The stopping and range of ions in solids*; Pergamon Press: New York, 1985.
(20) Fahey, P. M.; Griffin, P. B.; Plummer, J. D. *Rev. Mod. Phys.* **1989**, *61*, 289−384.
(21) Schoelkopf, R. J.; Wahlgren, P.; Kozhevnikov, A. A.; Delsing, P.; Prober, D. E. *Science* **1998**, *280*, 1238−1242.
(22) Buehler, T. M.; Chan, V.; Ferguson, A. J.; Dzurak, A. S.; Hudson, F. E.; Reilly, D. J.; Hamilton, A. R.; Clark, R. G.; Jamieson, D. N.; Yang, C.; Pakes, C. I.; Prawer, S. *Appl. Phys. Lett.* **2006**, *88*, 192101.
(23) Lee, K. H.; Greentree, A. D.; Dinale, J. P.; Escott, C. C.; Dzurak, A. S.; Clark, R. G. *Nanotechnology* **2005**, *16*, 74−81.
(24) Barrett, S. D.; Milburn, G. J. *Phys. Rev. B* **2003**, *68*, 155307.
(25) Hu, X.; Koiller, B.; Das Sarma, S. *Phys. Rev. B* **2005**, *71*, 235332.
(26) Wellard, C. J.; Hollenberg, L. C. L.; Das Sarma, S. *Phys. Rev. B* **2006**, *74*, 075306.
(27) Ralls, K. S.; Skocpol, W. J.; Jackel, L. D.; Howard, R. E.; Fetter, L. A.; Epworth, R. W.; Tennant, D. M. *Phys. Rev. Lett.* **1984**, *52*, 228−231.
(28) Poindexter, E. H. *Semicond. Sci. Technol.* **1989**, *4*, 961−969.

NL070797T